Heliyon 10 (2024) e30814

Contents lists available at ScienceDirect

Heliyon

journal homepage: www.cell.com/heliyon

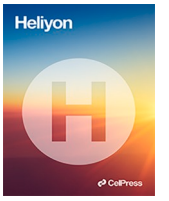

Research article

Mitochondrial ROS participates in *Porphyromonas gingivalis*-induced pyroptosis in cementoblasts

Weiman Sun [a,b], Tianrui Yang [a,b], Chenxu Wang [a,b], Houxuan Li [a], Lang Lei [a,*]

[a] *Nanjing Stomatological Hospital, Affiliated Hospital of Medical School, Research Institute of Stomatology, Nanjing University, Nanjing, China*
[b] *Central Laboratory of Stomatology, Nanjing Stomatological Hospital, Affiliated Hospital of Medical School, Research Institute of Stomatology, Nanjing University, Nanjing, China*

ARTICLE INFO

Keywords:
Cementoblasts
Pyroptosis
Mitochondrial ROS
Periodontology
Orthodontics

ABSTRACT

This study aimed to investigate correlation between mitochondrial reactive oxygen species and *Porphyromonas gingivalis* in the process of cementoblast pyroptosis. Lactate dehydrogenase activity assay, enzyme-linked immunosorbent assay, western blotting and flow cytometry analysis were utilized to explore whether *Porphyromonas gingivalis* triggered pyroptosis in cementoblasts. Reactive oxygen species and mitochondrial reactive oxygen species were detected using flow cytometry and fluorescence staining. The effect of mitochondrial reactive oxygen species on the *Porphyromonas gingivalis*-induced pyroptosis of cementoblasts was assessed by Mito-Tempo, mitochondrion-targeted superoxide dismutase mimetic. Phosphorylation levels of p65 were measured by western blotting. SC75741, a nuclear factor-kappa B inhibitor, was added to block the nuclear factor-kappa B in the *Porphyromonas gingivalis*-infected cementoblasts. *Porphyromonas gingivalis* triggered pyroptosis of cementoblasts, and an elevation in reactive oxygen species generation in the mitochondria was observed. Inhibition of mitochondrial reactive oxygen species reduced pyroptosis and nuclear factor-kappa B signaling pathway mediated the pyroptotic cell death in *Porphyromonas gingivalis*-infected cementoblasts. Together, our findings demonstrate that mitochondrial reactive oxygen species increased by *Porphyromonas gingivalis* participated in the pyroptosis of cementoblasts. Targeting mitochondrial reactive oxygen species may offer therapeutic strategies for root surface remodeling or periodontal regeneration.

1. Introduction

Cementum, covering the root surface, serves as a protective shield from bacteria and acids. It links the tooth to the alveolar bone,

Abbreviations: LPS, lipopolysaccharide; TLR, Toll-like receptor; RANKL, receptor activator of nuclear factor-kappa B ligand; ROS, reactive oxygen species; *P. gingivalis*, Porphyromonas gingivalis; NLRs, nod-like receptors; NLRP3, nod-like receptor family pyrin domain-containing 3; ASC, apoptosis-associated speck-like protein; GSDMD, gasdermin D; pro-IL-1β, pro-interleukin 1 beta; mtROS, mitochondrial reactive oxygen species; OD, optical density; NF-κB, nuclear factor-kappa B; LDH, Lactate Dehydrogenase Activity; ELISA, enzyme-linked immunosorbent assay; MOI, multiplicity of infection; MT, Mito-Tempo; p-p65, phospho-p65; NOXs, NADPH oxidase; MMP, mitochondrial membrane potential; IRAK3, interleukin 1 receptor-associated kinase 3; SOD, superoxide dismutase; PRXs, peroxiredoxins; UCP2, uncoupling protein 2.

* Corresponding author. Nanjing Stomatological Hospital, Affiliated Hospital of Medical School, Research Institute of Stomatology, Nanjing University, #30 Zhongyang Road, Nanjing, 210018, China.

E-mail addresses: weimsun1022@163.com (W. Sun), yyyouthrr@163.com (T. Yang), wcx1451110408@163.com (C. Wang), lihouxuan3435_0@163.com (H. Li), leilangdental@163.com (L. Lei).

https://doi.org/10.1016/j.heliyon.2024.e30814
Received 26 June 2023; Received in revised form 2 April 2024; Accepted 6 May 2024
Available online 7 May 2024

maintains the tooth's structural integrity, and ensures homeostasis of periodontal tissues [1]. Cementoblasts, lining on the root, secrete organic components of the cementum, such as bone sialoprotein, osteopontin and so on [2,3]. Such cementum-forming capacity is essential for the physiological root formation and in the pathological root repair during orthodontic tooth movement; therefore, a pool of viable cementoblasts is vital to balance the gain and loss in the periodontal niche in both physiologic and pathologic conditions [4]. In addition, cementoblasts contribute to the periodontal regeneration process by producing the newborn cementum that anchors the periodontal ligament, connecting the tooth with the alveolar bone [5,6].

As a type of vital resident cells within the periodontal membranes lining the root surfaces, cementoblasts are constantly irritated by bacterial stimuli from the biofilms in the periodontal pockets. After ligation with lipopolysaccharide (LPS), fimbriae and lipoteichoic acid, cementoblasts release inflammatory substances and osteoclastogenesis-associated molecule, such as interleukin 6 (IL-6) and matrix metalloproteinases [7–9]. Such inflammatory events not only inhibit the mineralization ability of cementoblasts, but also promote inflammatory resorption and enhance cellular oxidative stress [10–13].

Despite a host of literature regarding inflammatory responses of cementoblasts following bacterial stimuli, loss of cementoblasts by various regulated cell deaths, including apoptosis and pyroptosis, has been seldomly addressed. Cementoblasts have been observed to undergo reactive oxygen species (ROS)-related intrinsic apoptotic pathway following sodium fluoride stimulation [14]; in addition, it can also occur as the result of interleukin 1 beta (IL-1β) and compressive force [15,16]. Moreover, *Porphyromonas gingivalis* (*P. gingivalis*), crucial for the onset and advancement of periodontitis, promotes pyroptosis of cementoblasts by tet methylcytosine dioxygenase 1 and glycolysis [17–19]. Nevertheless, the process through which *P. gingivalis* triggers pyroptotic cell death remains incompletely understood.

In the classical pyroptotic pathway, activated nod-like receptors (NLRs), such as NLR family pyrin domain containing 3 (NLRP3), interact with apoptosis-associated speck-like protein containing a CARD (ASC), facilitating the recruitment and activation of pro-caspase 1. Subsequently, the NLRP3-ASC-caspase 1 complex, termed the inflammasome complex, further cleaves the gasdermin D (GSDMD) into C-terminal and N-terminal, causing pores formation, leading to ultimate cell lysis and leakage [20]. Furthermore, caspase 1 activation leads to the cleavage of pro-IL-1β and pro-IL-18, aiding in the development of the inflammatory cytokines IL-1β and IL-18 [21].

Mitochondria serve as a hub not only for energy production, but also for the generation of ROS during the energy generation process of oxidative phosphorylation [22]. Oxidative stress is a driving force in the onset of various cell death. Moreover, mitochondrial ROS (mtROS) may act as a priming signal for inflammasome activation [23]. Therefore, we hypothesized that mtROS induced by *P. gingivalis* promotes pyroptosis in cementoblasts.

2. Materials and methods

2.1. Cell culture and treatment

For this research, cementoblast cell line called OCCM-30 (RRID CVCL_D4XK) derived from mice was obtained from a biotechnology company named Mingzhoubio in China. As described by Xu et al., Cell culture was in Dulbecco's modified Eagle's medium (DMEM, Gibco, USA), and the culture medium was supplemented with 100 U/ml penicillin, 100 μg/ml streptomycin and 10 % (v/v) fetal bovine serum (FBS, Gibco, USA) [24]. .

2.2. Bacterial culture and drugs treatment

P. gingivalis, strain ATCC 33277, was maintained in the brain heart infusion broth, with supplement of yeast extract (1 mg/ml), hemin (5 mg/ml) and menadione (1 mg/ml) in an anaerobic condition (85 % N_2, 5 % H_2, and 10 % CO_2) at 37 °C. Bacterial levels were normalized using a spectrophotometer (SpectraMax M3, USA) to an optical density (OD) of 1 at 600 nm, equivalent to 10^9 CFU/ml [25]. *P. gingivalis* infected OCCM-30 cells at the exponential growth phase with varying multiplicity of infection (MOI = 30, 100 and 300) as detailed in the figure captions.

Mito-Tempo (MedChemExpress, USA), the mtROS scavenger, MCC950 (MedChemExpress, USA), the selective NLRP3 inhibitor, and SC75741 (Selleck, USA), the nuclear factor-kappa B (NF-κB) inhibitor were used at the concentration of 100 μM or 5 μM respectively for 2 h before the experiment.

2.3. Lactate dehydrogenase activity (LDH) assay

New medium with 1 % FBS was added after cementoblasts were cultured for 24 h. Apart from the experimental group, the culture wells were also divided into blank control, sample control, and lysis control (maximum enzyme activity). According to the experimental requirements, the corresponding treatments were applied. Cell lysis solution was added for 1 h before the assay. To assess the membrane integrity, culture medium of OCCM-30 cells was collected after treatment and assessed for LDH release using the assay kit from Beyotime in China as instructions. The relative quantification of LDH release levels were calculated as Peng et al. performed [17].

2.4. Annexin V-FITC/PI assay

2×10^5 cementoblasts were placed into 6-well plates. As described by Peng et al. [17], cells, digested with trypsin (without EDTA), along with culture supernatant, were collected in polypropylene FACS tubes. Following centrifugation, the cells were treated with PI

and Annexin V (Multisciences, China) following the protocols. Stained cells were quantified using FACS Calibur (BD Biosciences, USA) and analyzed with FlowJo software version 10.10.0 from Tree Star in the United States.

2.5. Enzyme-linked immunosorbent assay (ELISA)

Culture medium of OCCM-30 cells after treatment was collected, and sandwich ELISA (IL-1β, MultiSciences, China; IL-18, JYB, China) was used for quantification following the instruction of the manufacturer. The OD was read using a Spectra Max M3 (Molecular

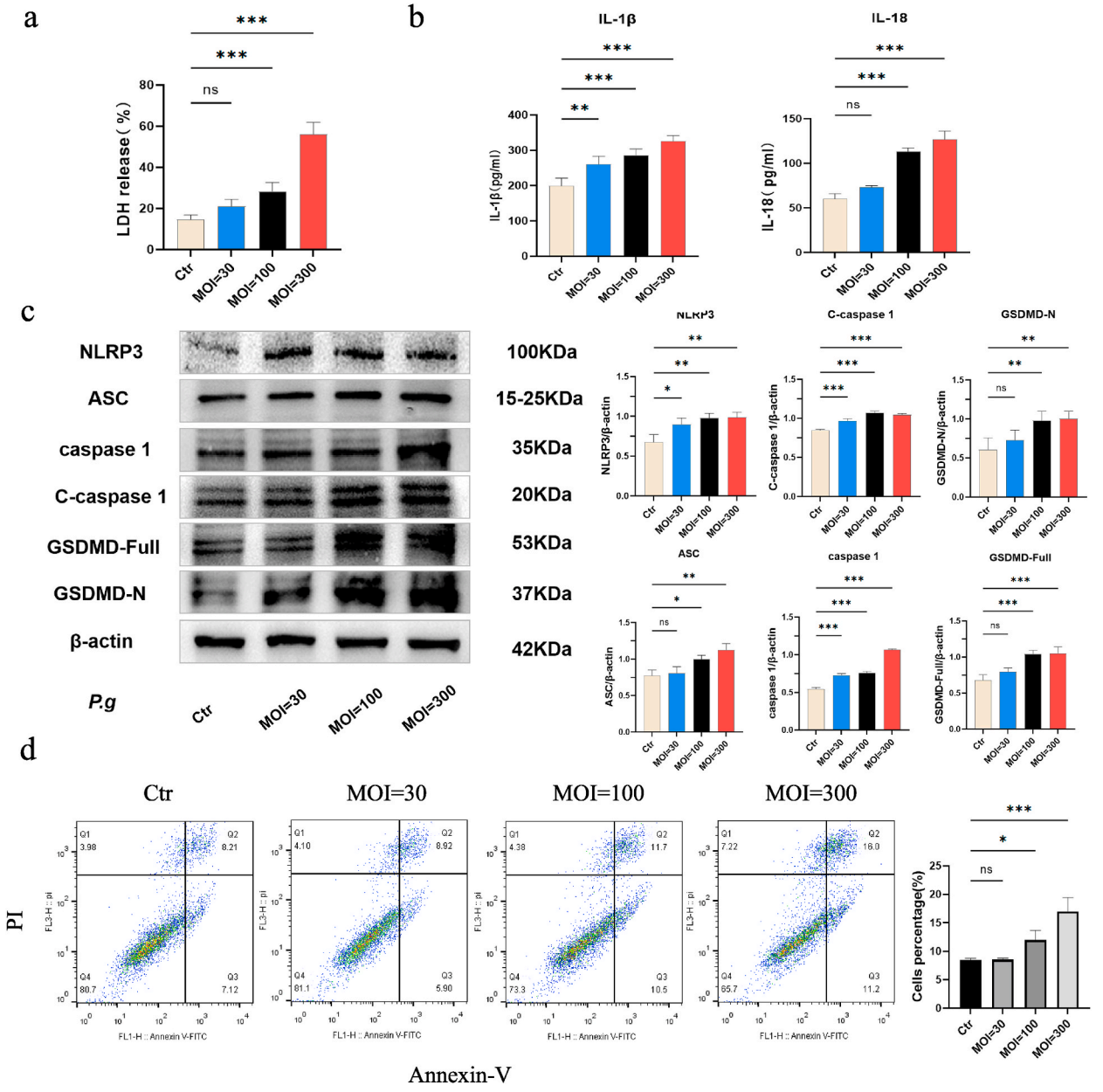

Fig. 1. *P. gingivalis* induced pyroptosis in OCCM-30 cells.
OCCM-30 cells were treated by MOI = 0, 30, 100 and 300 of *P. gingivalis* for 24 h. (a) Relative LDH release in the culture supernatants from OCCM-30 cells was measured. (b) IL-1β and IL-18 release in the culture medium were detected by ELISA. (c) Protein expression was analyzed by Western blot after bacterial infection. Data are expressed as relative ratios of specific proteins to β-actin (n = 3). More details were shown in the Supplemental Information S1. (d) OCCM-30 cells treated with *P. gingivalis* as indicated were measured by flow cytometry using an annexin V-FITC/PI detecting kit. Annexin V^+/PI^+ indicated the pyroptotic cells. Bar chart indicates the percentage of pyroptotic cells. Data were shown as mean ± standard deviation from three experiments independently. ***, $P < 0.001$; **, $P < 0.01$; *, $P < 0.05$. Ctr: control; MOI: multiplicity of infection; C-caspase 1: cleaved caspase 1; GSDMD-Full, gasdermin D-full length; GSDMD-N, gasdermin D-N terminal.

Devices, USA).

2.6. Western blot

OCCM-30 cells after treatment were collected with RIPA buffer (Beyotime, China) on the ice. Proteins were isolated using SDS-PAGE (SmartLifesciences, China), then moved to a PVDF membrane from Millipore in the USA. Following the use of QuickBlock™ blocking buffer (Beyotime, China) to block the PVDF membrane, the primary antibody specific to the target protein was added for

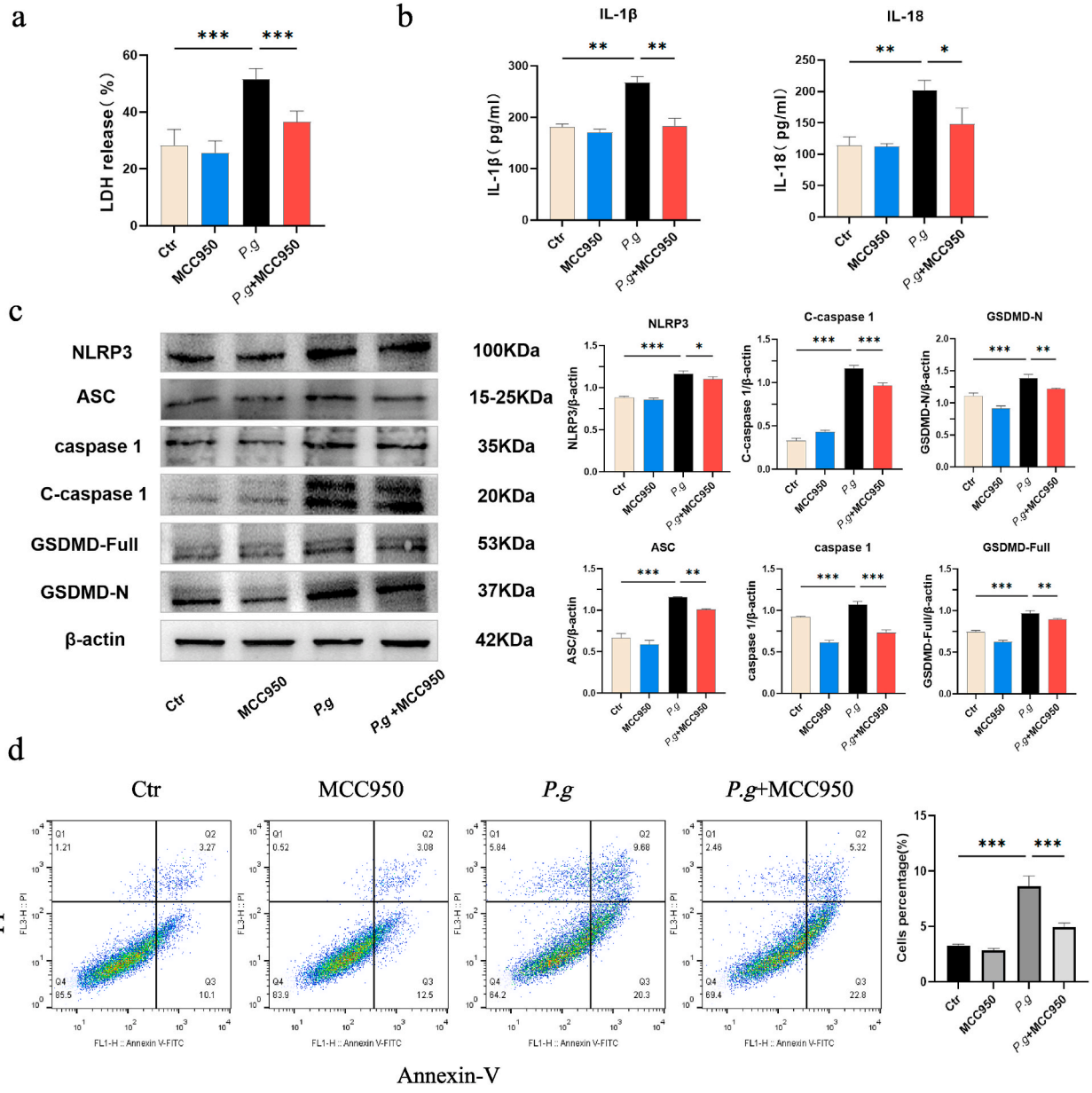

Fig. 2. *P. gingivalis* induced NLRP3 inflammasome-mediated pyroptosis of cementoblasts
OCCM-30 cells were preincubated with 5 μM MCC950 for 2 h and treated with *P. gingivalis* (MOI = 100) for 24 h. (a) Relative LDH release in OCCM-30 cells. (b) IL-1β and IL-18 release in the culture medium were detected by ELISA. (c) Protein expression was analyzed by Western blot after bacterial infection. Data are expressed as relative ratios of specific proteins toβ-actin (n = 3). More details were shown in the Supplemental Information S1. (d) OCCM-30 cells treated as indicated were measured by flow cytometry using an annexin V-FITC/PI apoptotic detecting kit. Annexin V^+/PI^+ indicated the pyroptotic cells. Bar chart indicates the percentage of pyroptotic cells. Data were shown as mean ± standard deviation from three experiments independently. ***, P < 0.001; **, P < 0.01; *, P < 0.05. Ctr: control; *P.g*: *Porphyromonas gingivalis*; C-caspase 1: cleaved caspase 1; GSDMD-Full, gasdermin D-full length; GSDMD-N, gasdermin D-N terminal.

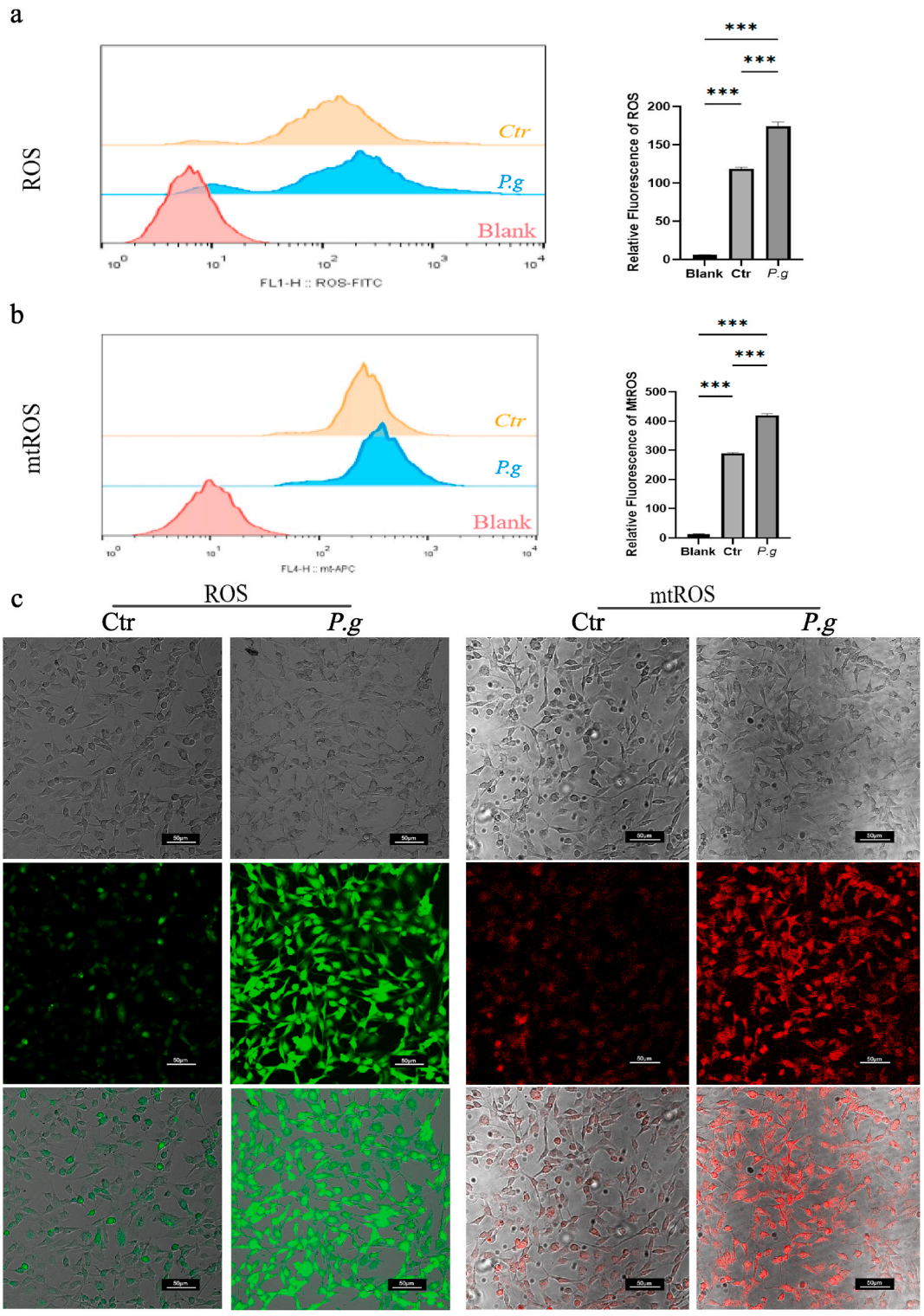

Fig. 3. *P. gingivalis* induced Mitochondrial ROS and ROS production in OCCM-30 cells
OCCM-30 cells were treated with *P. gingivalis* (MOI = 100) for 8 h. Mitochondrial ROS and ROS production were examined by flow cytometry (a, b) and immunofluorescence (c) by MitoSOX Deep Red and DCFH-DA. More details were shown in the Supplemental Information S2. ***, P < 0.001; **, P < 0.01; *, P < 0.05. Ctr: control; P.g: Porphyromonas gingivalis; ROS: reactive oxygen species; mtROS: mitochondrial ROS.

incubation. Rabbit anti-β-actin (CST, USA), rabbit anti-caspase 1 (CST, USA), anti-NLRP3 (Affinity, China), anti-GSDMD (Proteintech, China), anti-ASC (Abcam, UK), anti-phospho-p65 (CST, USA), and anti-p65 (CST, USA) were used in our experiment. The intact OD for the protein band was analyzed by the Image-J software (V1.8.0, National Institutes of Health, USA).

2.7. Mitochondrial ROS (mtROS) and ROS detection

MitoSOX Deep Red from DOJINDO in Japan and a kit from Beyotime Biotechnology in China were utilized for the measurement of

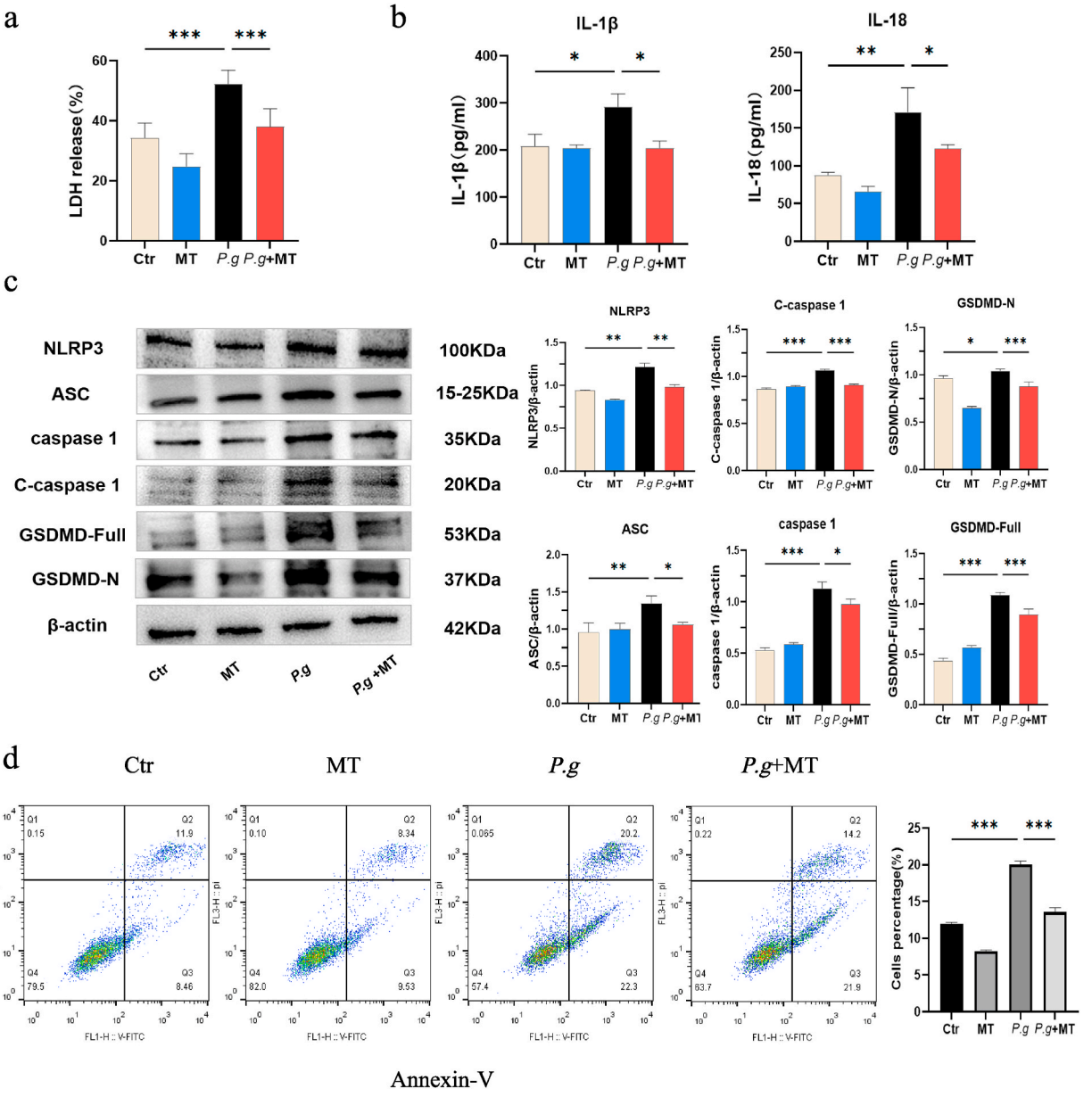

Fig. 4. MtROS participates in the pyroptosis induced by *P. gingivalis* in OCCM-30 cells
OCCM-30 cells were preincubated with 100 μM Mito-Tempo for 2 h and treated with *P. gingivalis* (MOI = 100) for 24 h. (a) Relative LDH release in OCCM-30 cells. (b) IL-1β and IL-18 release in the culture medium were detected by ELISA. (c) Protein expression was analyzed by Western blot after bacterial infection. Data are expressed as relative ratios of specific proteins to β-actin (n = 3). More details were shown in the Supplemental Information S1. (d) OCCM-30 cells treated as indicated were measured by flow cytometry using an annexin V-FITC/PI apoptotic detecting kit. Annexin V^+/PI^+ indicated the pyroptotic cells. Bar chart indicates the percentage of pyroptotic cells. Data were shown as mean ± standard deviation from three experiments independently. ***, $P < 0.001$; **, $P < 0.01$; *, $P < 0.05$. Ctr: control; MT: Mito-Tempo; *P.g*: *Porphyromonas gingivalis*; C-caspase 1: cleaved caspase 1; GSDMD-Full, gasdermin D-full length; GSDMD-N, gasdermin D-N terminal.

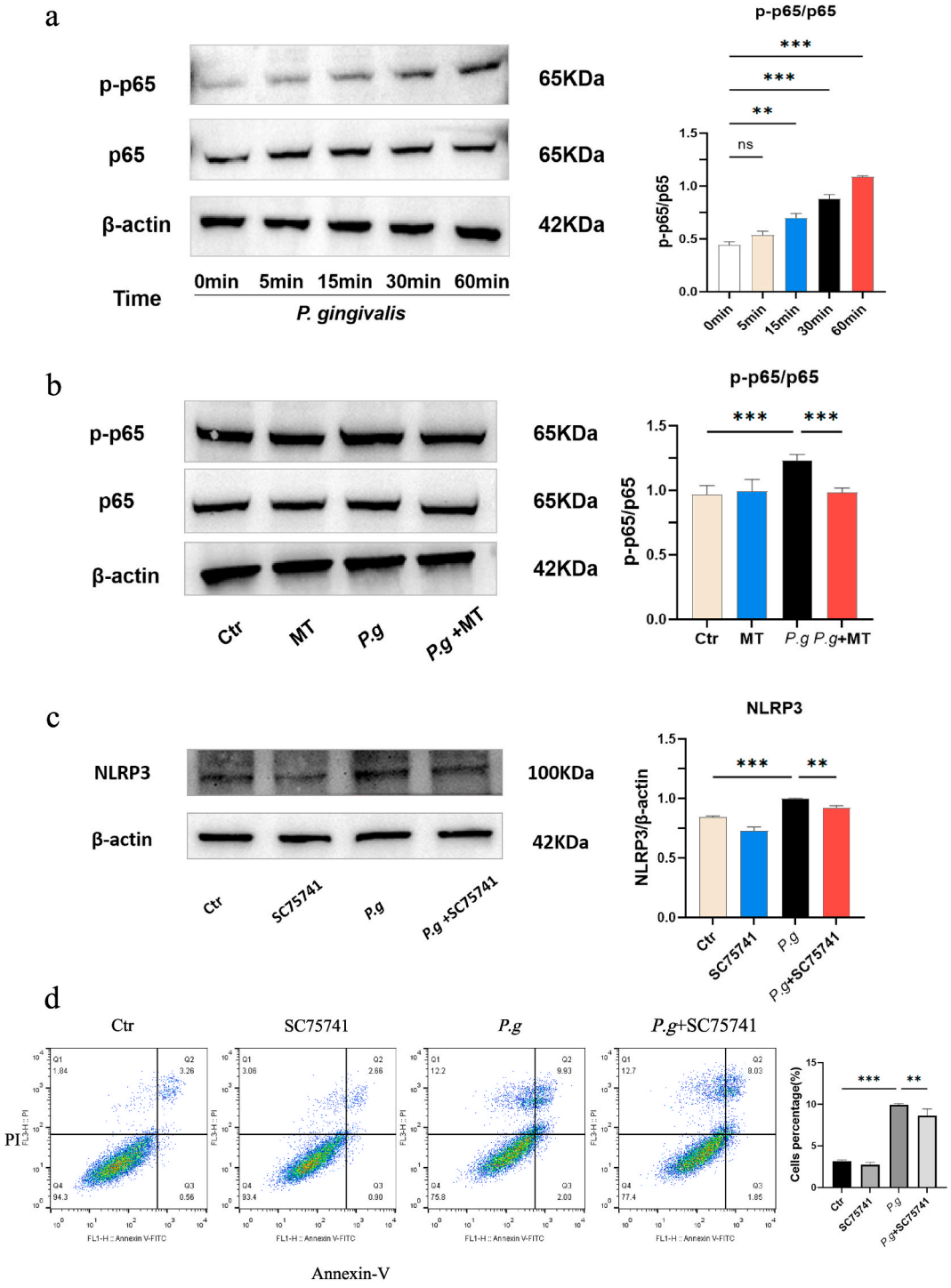

Fig. 5. Mitochondrial ROS induced pyroptosis through phospho-p65 in *P. gingivalis*-infected cementoblasts
(a) OCCM-30 cells time-dependently infected with *P. gingivalis* (MOI = 100). Protein expression was analyzed by Western blot after *P. gingivalis* infection (n = 3). (b) After preincubated with 100 μM Mito-Tempo, protein expression in OCCM-30 cells treated by *P. gingivalis* was analyzed by Western blot (n = 3). More details were shown in the Supplemental Information S1. After preincubated with 5 μM SC75741, protein expression (c) and Annexin V^+/PI^+ (d) of OCCM-30 cells treated by *P. gingivalis* were analyzed by Western blot and flow cytometry. Bar chart indicates the percentage of pyroptotic cells. Data were shown as mean ± standard deviation from three experiments independently. ***, $P < 0.001$; **, $P < 0.01$; *, $P < 0.05$. Ctr: control; MT: Mito-Tempo; *P.g & P. gingivalis*: *Porphyromonas gingivalis*.

mtROS and ROS accumulation.

Following an 8-h exposure to *P. gingivalis*, trypsin-digested cells washed with PBS were gathered in polypropylene FACS tubes. Incubation with 10 μM MitoSOX Deep Red and DCFH-DA reagent at 37 °C for 30 min. Detection of mtROS and ROS was performed on FACS Calibur (BD Biosciences, USA), and both the procedures and result analysis followed previous literature guidelines [26].

Confocal microscopy was used to analyze OCCM-30 cells, which were placed on a confocal dish and exposed to *P. gingivalis* for 8 h. Following a PBS wash, the cells were then exposed to 10 μM MitoSOX Deep Red and DCFH-DA reagent as above. Confocal microscopy (Nikon A1, Japan) was used to observe the production of mtROS and ROS.

2.8. Statistical analysis

The data were analyzed and graphed in the GraphPad Prism (V9.0, GraphPad Software Inc, USA). All data showed a normal contribution in the Shapiro-Wilk test. In addition, one-way ANOVA was used to explore the statistical difference, followed by the post-hoc multiple comparisons (Tukey). Values of $p < 0.05$ were considered statistically significant.

3. Results

3.1. Pyroptosis was triggered by P. gingivalis in OCCM-30 cells

P. gingivalis was used to stimulate cementoblasts at various MOI values (30, 100 and 300) for 24 h. We initially examined the amount of LDH released from the treated OCCM-30 cells, which revealed that *P. gingivalis* significantly increased the LDH release levels ($P < 0.001$, Fig. 1a). Moreover, we also detected elevated levels of IL-1β and IL-18 in the supernatant after *P. gingivalis* treatment, which were proportionate to the dosage (Fig. 1b). Meanwhile, *P. gingivalis* upregulated the protein expression of pyroptosis-associated molecules. As demonstrated in Fig. 1c and Supplemental Information S1, pyroptosis-related protein was increased in the cementoblasts. In addition, a notable rise of cells in the proportion of both positive of annexin V and PI after treatment, indicating that *P. gingivalis* promotes cell death in OCCM-30 cells ($P < 0.001$, Fig. 1d).

3.2. P. gingivalis induced NLRP3 inflammasome-mediated pyroptosis of cementoblasts

To further investigate whether *P. gingivalis* infection affects NLRP3 expression in cementoblasts, the specific NLRP3 inhibitor, MCC950, was used. The MCC950 administration significantly inhibited the *P. gingivalis*-induced release of LDH in OCCM-30 cells (Fig. 2a). MCC950 pretreatment significantly reduced IL-1β and IL-18 levels (Fig. 2b) and proteins expression (Fig. 2c & Supplemental Information S1) ($P < 0.05$). Moreover, it also revealed a reduction in the double positive (annexin V+/PI $^{+}$) cell rate after treatment of MCC950 ($P < 0.001$) (Fig. 2d). Thus, we conclude that *P. gingivalis* induces pyroptosis by activating the NLRP3.

3.3. Mitochondrial ROS participates in P. gingivalis-induced pyroptosis in cementoblasts

After 8 h of stimulation with *P. gingivalis*, OCCM-30 cells exhibited a notable rise ($P < 0.001$) in ROS and mtROS expression as detected by fluorescence staining and flow cytometry (Fig. 3a, b, c and Supplemental Information S2), suggesting the induction of oxidative stress by *P. gingivalis*.

To confirm the involvement of mtROS in *P. gingivalis*-triggered pyroptosis, cementoblasts were pretreated with 100 μM Mito-Tempo (MT) for 2 h. Compared to the group only exposed to *P. gingivalis*, cells treated with Mito-Tempo prior to *P. gingivalis* had significantly decreased the LDH release levels (Fig. 4a). In addition, inhibition of mtROS suppressed IL-1β and IL-18 in cementoblasts ($P < 0.05$, Fig. 4b). Pyroptosis-related protein was decreased following treatment with Mito-Tempo (Fig. 4c & Supplemental Information S1). Furthermore, flow cytometric analysis showed that double positive cell rate was decreased after pretreatment of Mito-Tempo ($P < 0.001$, Fig. 4d). Together, it indicates that inhibition of mtROS reduces *P. gingivalis*-induced pyroptosis.

3.4. Mitochondrial ROS induced pyroptosis through phospho-p65 in P. gingivalis-infected cementoblasts

After treatment of *P. gingivalis*, phospho-p65 (p-p65) levels were significantly upregulated compared to non-phosphorylated levels in a time-dependent manner (Fig. 5a & Supplemental Information S1). Preincubation with 100 μM Mito-Tempo was found to inhibit levels of p-p65 ($P < 0.001$, Fig. 5b & Supplemental Information S1). Furthermore, after using 5 μM SC75741, the NF-κB inhibitor, the expression of NLRP3 (Fig. 5c & Supplemental Information S1) and cell rate of both annexin V+and PI+(Fig. 5d) were decreased ($P < 0.01$). Thus, we conclude that mtROS induced pyroptosis by activating the NF-κB pathway.

4. Discussion

Life or death is a critical fate in host cells during the combat against microbes. *P. gingivalis* may induce pro-inflammatory events in osteoblasts, including cytokine release and RANKL production. In our study, *P. gingivalis* induced pyroptosis in cementoblasts. The upregulation of mtROS contribute to the onset pyroptosis in cementoblasts. Targeting mtROS-related pyroptosis offers a possible strategy for the viability of cementoblasts and the integrity of the cementum.

Cementoblasts, with the capacity of matrix deposition and mineralization, are essential for root resorption repairs and periodontal

regeneration [5,27]. *P. gingivalis* and its LPS inhibited cementoblasts mineralization and induced inflammatory responses and the up-regulation of oxidative stress [9,28]. OCCM-30 cells are murine-derived immortalized cementoblast cell line containing toll-like receptors 2/4(TLR2/4) [7,8]. Some virulence factors present in *P. gingivalis*, such as LPS and fimbriae are recognized by TLRs during infection, and subsequently trigger the NF-κB to upregulate the expression of NLRs [29–32]. In our present experiment, cementoblasts treated with *P. gingivalis* were showed dose-dependent increases in the double positive cell rate and the amount of LDH released, suggesting lytic cell death. Further, the expression levels of actived-caspase 1 and GSDMD-N increased, indicating that pyroptosis occurs. Moreover, by using NLRP3 inhibitor MCC950, pyroptosis related index were reversed. It showed that *P. gingivalis* may induce pyroptosis by activating NLRP3 inflammasome.

Mitochondria are main sites of intracellular oxidative phosphorylation to produce ATP and are major sources of intracellular ROS [33]. Currently, there is a belief that the electron transport chain in mitochondria is crucial in generating intracellular ROS, which in turn can activate NOXs and elevate levels of ROS within cells [34]. Extensive evidence suggests that *P. gingivalis* or LPS causes oxidative stress and mitochondrial dysfunction, finally leading to inevitable damage [35,36]. In gingival fibroblasts and periodontal ligament cells, *P. gingivalis*-LPS infection leads to mtROS generation, mitochondrial membrane potential (MMP) loss, and mitochondrial biogenesis [37–40]. Similarly, increases in mtROS and ROS generation were observed in cementoblasts after treatment with *P. gingivalis,* indicating that *P. gingivalis* may cause mitochondrial disorder and oxidative stress in OCCM-30 cells.

Mitochondria in regulating the pyroptosis has attracted wide attention. Studies have shown that mitochondria have the ability to regulate NLRP3 inflammasome activation through multiple mechanisms [41]. As byproducts of mitochondrial energy metabolism, mtROS have also been thought as an intermediate in triggering the inflammatory signalling cascade and activating the NLRP3 to enhance the pyroptosis [42,43]. In our study, inhibition of mtROS by Mito-Tempo reduced pyroptosis in cementoblasts. It demonstrated that mtROS may partly participate in *P. gingivalis*-induced pyroptosis in cementoblasts. Moreover, it should be noted that NOX, eNOS uncoupling and xanthine oxidase can also regulate its production [44]. Liu et al. found that hyperhomocysteinemia (HHcy) promoted the NOX complex production, which increases ROS levels, inflammasome activation, and pyroptosis [45]. It has been reported that NOX/ROS signalling pathways are able to trigger oxygen sensitivity in the inflammasome, leading to pyroptosis in hematopoietic stem cells [46]. Cellular ROS was thoughted to induce pyroptosis via triggering NLRP3 inflammasome activation by two steps: related gene transcription and translation [47], and the activation of inflammasome through TXNIP [48]. Further investigation may be needed to performed to explore the role of other sources of ROS in cementoblasts.

NF-κB is crucial in regulating inflammatory responses and the activation of p65 has been implicated in the onset of pyroptosis [43,49]. Our research found that *P. gingivalis* triggered the activation of p-p65. Meanwhile, suppression of mtROS inhibited activation of p-p65 and cell death, indicating that NF-κB pathway activation may be the downstream point of mtROS. However, the process by which mtROS regulates NF-κB signalling is not totally clarified. Some researchers have proposed that interleukin 1 receptor-associated kinase 3 (IRAK3) acts in the upstream of NF-κB, blocking IRAK1 and IRAK4 separation from MyD88 [50,51]. In addition, Jin et al. reported that Ginsenoside Rh1 suppresses NF-κB by deactivating STAT3 through mtROS [52]. Further investigation may be necessary to determine whether overproduced mtROS or ROS can act on this key enzyme or upstream pathway, thereby activating NF-κB signaling.

Although we have observed that inhibiting mtROS reduces pyroptosis in cementoblasts, further studies are still needed to explore how *P. gingivalis* increase the production of mtROS, and how to reduce pyroptosis of cementoblasts. *P. gingivalis* induces mitochondrial fragmentation and raises the mtROS production in vascular endothelial cells [53]. Mitophagy which removes damaged mitochondria can reduce the production of mtROS in periodontitis [26]. Moreover, to maintain the balance of mtROS, mitochondria are equipped with scavenging systems, such as superoxide dismutase (SOD), peroxiredoxins (PRXs), uncoupling protein 2 (UCP2) and so on. Reduced activity of these scavenging systems has been implicated in the increase of mtROS and pathological injury observed in diabetic, liver, kidney and cardiovascular diseases [54–57]. Whether such regulations of mtROS occur in the pathological role of *P. gingivalis* in cementoblasts deserves to be investigated. Additionally, certain newly developed substances have shown to have a notable impact on the oral ecosystem [58]. Lysates and postbiotics have the potential to alter clinical and microbiological factors in patients with periodontal disease. Therefore, these products should be included as adjuvants in future clinical studies, especially in situations involving *P. gingivalis*-induced pyroptosis [59,60].

4.1. Limitation

However, our study still has several limitations. Given that *P. gingivalis* contains multiple virulence factors, including LPS, gingipains and outer membrane vesicles, their respective effects on mtROS and pyroptosis are still needed to be further revealed. The establishment of animal model is necessary to better unveil the pathological role of mtROS on the cementum destruction or formation during *P. gingivalis* infection.

5. Conclusion

In conclusion, the findings of this study suggest that mtROS participates in the NLRP3 inflammasome-dependent pyroptosis and the activation of p65. Targeting mtROS may hold promise for cementum regeneration and reconstruction.

Ethics declarations

This study was reviewed and approved by the Ethical Committee of Nanjing Stomatological Hospital, Medical School of Nanjing

University, with the approval number: NJSH-2023NL-27. Informed consent was not required for this study because no participants/patients were included in our study.

Funding statement

This study was supported by grants from Nanjing Medical Science and Technique Development Foundation (QRX17025 & QRX17081) and Nanjing Clinical Research Center for Oral Diseases (No.2019060009).

Data availability statement

All data used in the generation of the results presented in this manuscript will be made available upon reasonable request from the corresponding author.

CRediT authorship contribution statement

Weiman Sun: Writing – original draft, Validation, Methodology, Investigation, Formal analysis, Data curation. **Tianrui Yang:** Writing – original draft, Validation, Formal analysis, Data curation. **Chenxu Wang:** Writing – original draft, Validation, Formal analysis, Data curation. **Houxuan Li:** Writing – review & editing, Supervision, Funding acquisition, Conceptualization. **Lang Lei:** Writing – review & editing, Supervision, Funding acquisition, Conceptualization.

Declaration of competing interest

The authors declare that they have no known competing financial interests or personal relationships that could have appeared to influence the work reported in this paper.

Appendix A. Supplementary data

Supplementary data to this article can be found online at https://doi.org/10.1016/j.heliyon.2024.e30814.

References

[1] B.L. Foster, On the discovery of cementum, J. Periodontal. Res. 52 (4) (2017) 666–685.
[2] A. Hirata, T. Sugahara, H. Nakamura, Localization of runx2, osterix, and osteopontin in tooth root formation in rat molars, J. Histochem. Cytochem. 57 (4) (2009) 397–403.
[3] F.H. Nociti Jr., et al., Vitamin D represses dentin matrix protein 1 in cementoblasts and osteocytes, J. Dent. Res. 93 (2) (2014) 148–154.
[4] J. Zhao, et al., Stem cell contributions to cementoblast differentiation in healthy periodontal ligament and periodontitis, Stem Cell. 39 (1) (2021) 92–102.
[5] H. Arzate, M. Zeichner-David, G. Mercado-Celis, Cementum proteins: role in cementogenesis, biomineralization, periodontium formation and regeneration, Periodontol 67 (1) (2000) 211–233, 2015.
[6] W.J. Grzesik, A.S. Narayanan, Cementum and periodontal wound healing and regeneration, Crit. Rev. Oral Biol. Med. 13 (6) (2002) 474–484.
[7] E. Nemoto, et al., Regulation of cementoblast function by P. gingivalis lipopolysaccharide via TLR2, J. Dent. Res. 85 (8) (2006) 733–738.
[8] F.H. Nociti Jr., et al., Cementoblast gene expression is regulated by Porphyromonas gingivalis lipopolysaccharide partially via toll-like receptor-4/MD-2, J. Dent. Res. 83 (8) (2004) 602–607.
[9] S.B. Bozkurt, I. Tuncer Gokdag, S.S. Hakki, Porphyromonas gingivalis-Lipopolysaccharide induces cytokines and enzymes of the mouse cementoblasts, Cytokine 138 (2021) 155380.
[10] Y.Y. Zhang, et al., Cementogenesis is inhibited under a mechanical static compressive force via Piezo1, Angle Orthod. 87 (4) (2017) 618–624.
[11] H. Wang, et al., PGC-1 alpha regulates mitochondrial biogenesis to ameliorate hypoxia-inhibited cementoblast mineralization, Ann. N. Y. Acad. Sci. 1516 (1) (2022) 300–311.
[12] Y. Mada, et al., Effects of endogenous and exogenous prostaglandin E2 on the proliferation and differentiation of a mouse cementoblast cell line (OCCM-30), J. Periodontol. 77 (12) (2006) 2051–2058.
[13] K. Diercke, et al., Human primary cementoblasts respond to combined IL-1β stimulation and compression with an impaired BSP and CEMP-1 expression, Eur. J. Cell Biol. 91 (5) (2012) 402–412.
[14] J. Ni, et al., Sodium fluoride causes oxidative stress and apoptosis in cementoblasts, Chem. Biol. Interact. 294 (2018) 34–39.
[15] K. Diercke, et al., Gene expression profile of compressed primary human cementoblasts before and after IL-1β stimulation, Clin. Oral Invest. 18 (8) (2014) 1925–1939.
[16] Y. Yang, et al., Compressive force regulates cementoblast migration via downregulation of autophagy, J. Periodontol. 92 (11) (2021) 128–138.
[17] Y. Peng, et al., Tet methylcytosine dioxygenase 1 modulates Porphyromonas gingivalis-triggered pyroptosis by regulating glycolysis in cementoblasts, Ann. N. Y. Acad. Sci. 1523 (1) (2023) 119–134.
[18] W. Xu, et al., Roles of Porphyromonas gingivalis and its virulence factors in periodontitis, Adv Protein Chem Struct Biol 120 (2020) 45–84.
[19] L. Fiorillo, et al., Porphyromonas gingivalis, periodontal and systemic implications: a systematic review, Dent. J. 7 (4) (2019).
[20] A.N.R. Weber, et al., Recent insights into the regulatory networks of NLRP3 inflammasome activation, J. Cell Sci. 133 (23) (2020).
[21] J. Shi, W. Gao, F. Shao, Pyroptosis: gasdermin-mediated programmed necrotic cell death, Trends Biochem. Sci. 42 (4) (2017) 245–254.
[22] D.B. Zorov, M. Juhaszova, S.J. Sollott, Mitochondrial reactive oxygen species (ROS) and ROS-induced ROS release, Physiol. Rev. 94 (3) (2014) 909–950.
[23] Y. Wang, et al., Mitochondrial ROS promote macrophage pyroptosis by inducing GSDMD oxidation, J. Mol. Cell Biol. 11 (12) (2019) 1069–1082.
[24] L. Xu, et al., L-arginine protects cementoblasts against hypoxia-induced apoptosis through Sirt1-enhanced autophagy, J. Periodontol. 93 (12) (2022) 1961–1973.
[25] W. Su, et al., Hexokinase 2-mediated glycolysis supports inflammatory responses to Porphyromonas gingivalis in gingival fibroblasts, BMC Oral Health 23 (1) (2023) 103.

[26] K. Jiang, et al., PINK1-mediated mitophagy reduced inflammatory responses to Porphyromonas gingivalis in macrophages, Oral Dis. (2022).
[27] J. Liu, et al., Periodontal bone-ligament-cementum regeneration via scaffolds and stem cells, Cells 8 (6) (2019).
[28] X. Huang, et al., Ckip-1 mediates P. Gingivalis-suppressed cementoblast mineralization, J. Dent. Res. 101 (5) (2022) 599–608.
[29] N. Bostanci, G.N. Belibasakis, Porphyromonas gingivalis: an invasive and evasive opportunistic oral pathogen, FEMS Microbiol. Lett. 333 (1) (2012) 1–9.
[30] K.V. Swanson, M. Deng, J.P. Ting, The NLRP3 inflammasome: molecular activation and regulation to therapeutics, Nat. Rev. Immunol. 19 (8) (2019) 477–489.
[31] Y.Y. Li, et al., The effect of Porphyromonas gingivalis lipopolysaccharide on the pyroptosis of gingival fibroblasts, Inflammation 44 (3) (2021) 846–858.
[32] L. Wang, et al., Microtubule affinity regulating kinase 4 promoted activation of the NLRP3 inflammasome-mediated pyroptosis in periodontitis, J. Oral Microbiol. 14 (1) (2022) 2015130.
[33] V.G. Grivennikova, A.D. Vinogradov, Mitochondrial production of reactive oxygen species, Biochemistry (Mosc.) 78 (13) (2013) 1490–1511.
[34] M. Muñoz, et al., Differential contribution of Nox1, Nox2 and Nox4 to kidney vascular oxidative stress and endothelial dysfunction in obesity, Redox Biol. 28 (2020) 101330.
[35] P. Bullón, et al., Lipophilic antioxidants prevent lipopolysaccharide-induced mitochondrial dysfunction through mitochondrial biogenesis improvement, Pharmacol. Res. 91 (2015) 1–8.
[36] J. Liu, et al., Mitochondrial DNA efflux maintained in gingival fibroblasts of patients with periodontitis through ROS/mPTP pathway, Oxid. Med. Cell. Longev. 2022 (2022) 1000213.
[37] X. Li, et al., Mitochondrial reactive oxygen species mediate the lipopolysaccharide-induced pro-inflammatory response in human gingival fibroblasts, Exp. Cell Res. 347 (1) (2016) 212–221.
[38] K. Chu, et al., Ginsenoside Rg1 alleviates lipopolysaccharide-induced pyroptosis in human periodontal ligament cells via inhibiting Drp1-mediated mitochondrial fission, Arch. Oral Biol. 147 (2023) 105632.
[39] J. Liu, et al., Abnormal mitochondrial structure and function are retained in gingival tissues and human gingival fibroblasts from patients with chronic periodontitis, J. Periodontal. Res. 57 (1) (2022) 94–103.
[40] J.M. Suski, et al., Relation between mitochondrial membrane potential and ROS formation, Methods Mol. Biol. 810 (2012) 183–205.
[41] R. Zhou, et al., A role for mitochondria in NLRP3 inflammasome activation, Nature 469 (7329) (2011) 221–225.
[42] A.V. Kozlov, et al., Mitochondria-meditated pathways of organ failure upon inflammation, Redox Biol. 13 (2017) 170–181.
[43] W. Zhao, et al., Prototheca spp. induce an inflammatory response via mtROS-mediated activation of NF-κB and NLRP3 inflammasome pathways in bovine mammary epithelial cell cultures, Vet. Res. 52 (1) (2021) 144.
[44] Y. Liao, et al., NADPH oxidase 4 and endothelial nitric oxide synthase contribute to endothelial dysfunction mediated by histone methylations in metabolic memory, Free Radic. Biol. Med. 115 (2018) 383–394.
[45] S. Liu, et al., HHcy induces pyroptosis and atherosclerosis via the lipid raft-mediated NOX-ROS-NLRP3 inflammasome pathway in apoE(-/-) mice, Cells 11 (15) (2022).
[46] Y. Lin, Q.P. Gao, B.X. Ye, [Research progress on the role of pyroptosis in the pathogenesis of myelodysplastic syndrome -review], Zhongguo Shi Yan Xue Ye Xue Za Zhi 26 (3) (2018) 937–941.
[47] J.M. Abais, et al., Redox regulation of NLRP3 inflammasomes: ROS as trigger or effector? Antioxidants Redox Signal. 22 (13) (2015) 1111–1129.
[48] D. Zheng, et al., ROS-triggered endothelial cell death mechanisms: focus on pyroptosis, parthanatos, and ferroptosis, Front. Immunol. 13 (2022) 1039241.
[49] M.S. Hayden, S. Ghosh, Shared principles in NF-kappaB signaling, Cell 132 (3) (2008) 344–362.
[50] M. Hulsmans, et al., Interleukin-1 receptor-associated kinase-3 is a key inhibitor of inflammation in obesity and metabolic syndrome, PLoS One 7 (1) (2012) e30414.
[51] M. Hulsmans, E. Van Dooren, P. Holvoet, Mitochondrial reactive oxygen species and risk of atherosclerosis, Curr. Atherosclerosis Rep. 14 (3) (2012) 264–276.
[52] Y. Jin, et al., Ginsenoside Rh1 prevents migration and invasion through mitochondrial ROS-mediated inhibition of STAT3/NF-κB signaling in MDA-MB-231 cells, Int. J. Mol. Sci. 22 (19) (2021).
[53] T. Xu, et al., Porphyromonas gingivalis infection promotes mitochondrial dysfunction through Drp1-dependent mitochondrial fission in endothelial cells, Int. J. Oral Sci. 13 (1) (2021) 28.
[54] Y. Wang, et al., Peroxiredoxin 3 inhibits acetaminophen-induced liver pyroptosis through the regulation of mitochondrial ROS, Front. Immunol. 12 (2021) 652782.
[55] M.E. Widlansky, R.B. Hill, Mitochondrial regulation of diabetic vascular disease: an emerging opportunity, Transl. Res. 202 (2018) 83–98.
[56] J. Huang, et al., Upregulation of UCP2 expression protects against LPS-induced oxidative stress and apoptosis in cardiomyocytes, Oxid. Med. Cell. Longev. 2019 (2019) 2758262.
[57] M. Zhu, et al., AMPK activation coupling SENP1-Sirt3 axis protects against acute kidney injury, Mol. Ther. 31 (10) (2023) 3052–3066.
[58] M. Corsalini, et al., Non-surgical therapy and oral microbiota features in peri-implant complications: a brief narrative review, Healthcare 11 (5) (2023).
[59] A. Butera, et al., Evaluation of adjuvant systems in non-surgical peri-implant treatment: a literature review, Healthcare 10 (5) (2022).
[60] S. Shanbhag, et al., Spheroid coculture of human gingiva-derived progenitor cells with endothelial cells in modified platelet lysate hydrogels, Front. Bioeng. Biotechnol. 9 (2021) 739225.